Supplementary

Climate impact of contrail cirrus from hydrogen aircraft

Susanne Pettersson[1]*, Christian Azar[1], Daniel Johansson[1]

S1 Parameter settings for implementation of model developed by Kärcher et. al. (2015)

To implement and run the model developed by Kärcher et. al. [1] (subsequently referred to as K15) it needs to be parametrized. The chosen parameter values are listed in Table S1 below with short remarks, followed by the expressions mentioned in the remarks.

Table S1: Parameter settings needed for the K15 model and our base setting.

Parameter	Notation	Value	Unit	Comment
Water mass emission index for H_2	EI_{H_2O,H_2}	8.96	kg (kg fuel)$^{-1}$	
Water mass emission index for jet	$EI_{H_2O,J}$	1.23	kg (kg fuel)$^{-1}$	
Lubrication oil mass emission index	EI_o	2	mg (kg fuel)$^{-1}$	
Specific combustion heat H_2	Q_{H_2}	122.8	MJ (kg fuel)$^{-1}$	
Specific combustion heat jet A1	Q_J	43.2	MJ (kg fuel)$^{-1}$	
Propulsion efficiency hydrogen	η	0.44	-	[2], correspondence with Carlos Xisto
Air-to-fuel ratio at engine exit hydrogen	N_0	110	-	[2], correspondence with Carlos Xisto
Temperature of exhaust at time zero hydrogen	T_0	660	K	[2], correspondence with Carlos Xisto
Geometric mean radius of ambient aerosols	μ_a	15	nm	[1], [3], [4]
Standard deviation of ambient aerosols	σ_a	2.2	nm	[1]
Density of water	ρ_w	999.8	kg m^{-3}	Used for Kelvin radius in r_{act}, at 273 K
Surface tension of water	$\sigma_{s/a}$	0.0723	J m^{-2}	[5], used for Kelvin radius in r_{act}
Hygroscopicity parameter lubrication oil	κ_o	0.0006	-	[6]
Hygroscopicity parameter ambient aerosol	κ_a	0.5	-	[3], [1]
Ambient aerosol number concentration	n_a	1000	m^{-3}	high concentration
Density of lubrication oil	ρ_o	925	kg m^{-3}	[7], [8] used for number emission index
Molar mass air	M_{air}	0.0290	kg mole^{-1}	
Initial plume radius	r_0	0.5	m	[9], [1], used for plume cooling rate
Turbulent diffusivity	ϵ	0.0285	-	from experimental data [1] ([10]), used for plume cooling rate
Exit speed of exhaust	u_0	400	m s^{-1}	[1], used for plume cooling rate
Dilution parameter	β	0.9	-	[11], used for plume cooling rate

Kelvin radius:

$$r_k = \frac{4\sigma_{s/a} M_{water}}{R_M T \rho_w} \tag{S1}$$

where, M_{water} is the molar mass of water (18.01528×10^{-3} kg Mole^{-1}) and R_M the universal molar gas constant (8.314463 J (Mole K)$^{-1}$). We have used a constant value of the Kelvin radius, fixing the temperature in the

[1]Department of Space, Earth and Environment, Chalmers University of Technology, Maskingränd 2, 412 58 Gothenburg, Sweden.

above expression to $T = 273K$ and corresponding density of water to $\rho_w = 999.8$ kg m^{-3}. This gives the Kelvin radius $r_k \approx 2.30 \times 10^{-9}$. In Kärcher the Kelvin radius is set to 1 nm and in [5] it is set to the expression according to Eq. (S1) with $T = 298.15$K. We chose a fixed value of the Kelvin radius as in K15 for simpler implementation. At our chosen temperature of $T = 273$K water droplet formation takes place in the plume as it is cooling to ambient conditions. The equation for plume cooling rate mentioned in Table (S1) can be found in [1] Eq. (10) and (14).

We calculate the number emission index for lubrication oil as in Eq. (7) in [1]

$$EI_{\mathrm{n,oil}} = \frac{3EI_o}{4\pi\rho_o\mu_o^3} e^{-(9/2)\mathrm{Ln}^2\sigma_o} \tag{S2}$$

where μ_o is the median of the lubrication oil lognormal size distribution and σ_o the standard deviation.

Further comments:

Ambient aerosol size distribution properties are chosen in line with the literature for similar models ([1], [3], [4]). Ambient aerosols come in a large span of sizes, hygroscopicities and ambient concentrations. We model ambient aerosols as a single mode lognormal size distribution with a quite large standard deviation to account for the large variation in ambient aerosols, in addition we choose a quite high hygroscopicity parameter value of $\kappa_a = 0.5$ and fixed ambient concentration of 1000 cm^{-3} to not underestimate the influence of ambient aerosols on ice particle formation.

Other relations needed to implement the K15 model and which approximations we have used are found in Table (S3) (all other formulas needed found in [1])

Table S2: Relations needed for implementation of K15 and which approximations we have used.

Phenomenon	Notation	Name	Reference
Saturation water vapour pressure	$e_w(T)$	Goff - Gratch approximation	[12, 13]
Mean thermal speed of water molecules	$v(T)$	Maxwell-Boltzmann	
Molar volume of supercooled water	$M_\nu(T)$	-	
Latent heat evaporation	$L_w(T)$	-	[14]

S2 Activation radius correction

We added a factor to the expression for "dry" activation radius in Kärcher et. al. [1] to account for the worse fit for small κ-values like that of lubrication oil,

$$r_{act} = s^{-2/3}\frac{r_k}{(54\kappa)^{1/3}} \quad \rightarrow \quad \alpha_0\kappa^{\alpha_1}s^{-2/3}\frac{r_k}{(54\kappa)^{1/3}}, \tag{S3}$$

where r_k is the Kelvin radius from Eq. (S1). The functional form $\alpha_0\kappa^{\alpha_1}$ was found by visual inspection from corrections to improve the approximation to the actual relation which is at the local maximum (critical saturation ratio) of the Kappa-Köhler equation

$$S(r) = \frac{r^3 - r_d^3}{r^3 - r_d^3(1-\kappa)}\exp\left(\frac{4\sigma_{s/a}M_w}{RT\rho_w r}\right). \tag{S4}$$

The local maxima for varying dry radii, r_d, was found using Wolfram Mathematicas FindMaxima function. With the functional form the parameters $\alpha_0 = 1.16788$ and $\alpha_1 = 0.186086$ where then found with Wolfram Mathematica function FindFit which uses a least squares solution. The fit was calibrated such that the $\alpha_0\kappa^{\alpha_1} \approx 1$ at $\kappa = 0.5$ since no correction is needed for larger values of κ. Figure S1 below shows our fit compared to the original approximation in Eq. (S3) and the critical saturation ratio found from the κ-Köhler equation S4.

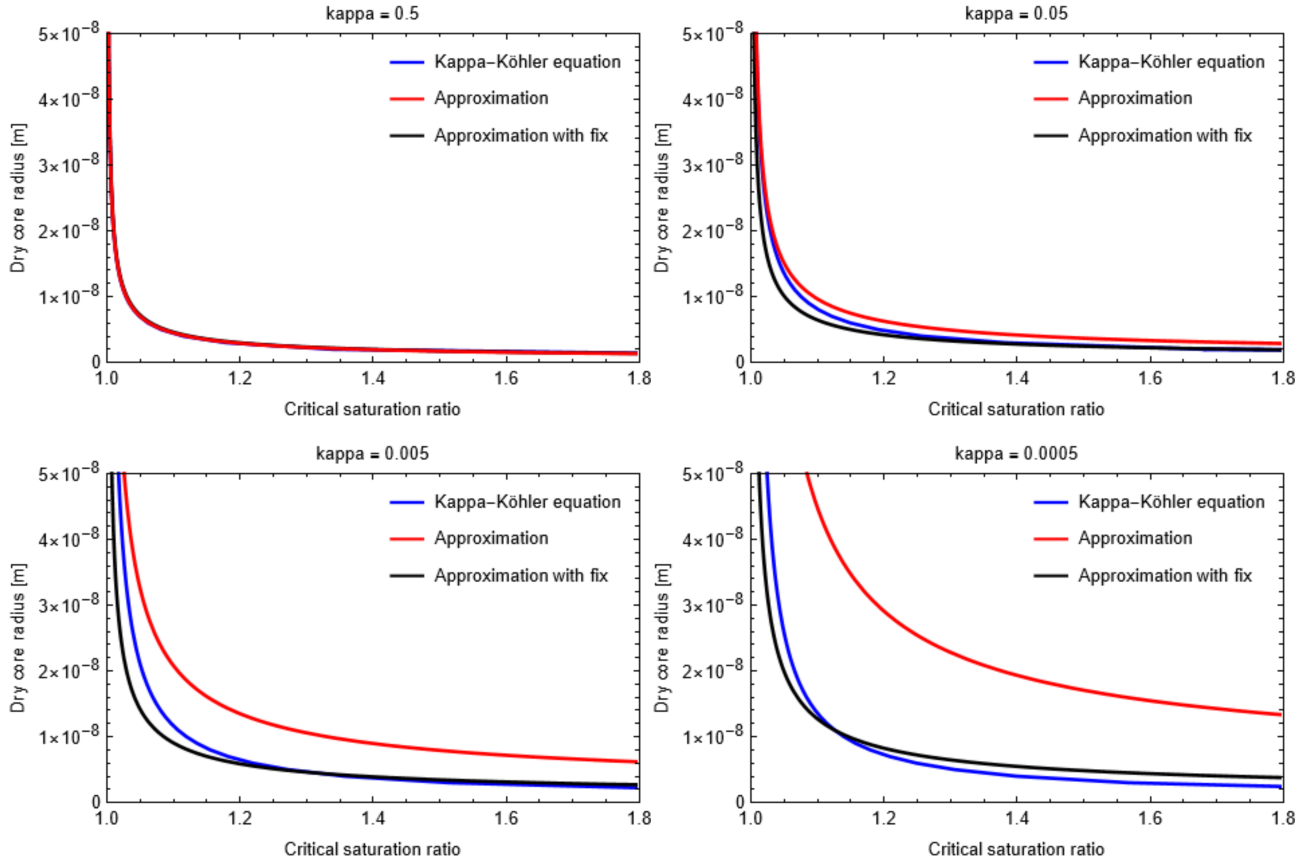

Illustration of how well our approximate fit (black line) and the approximate fit by [1] (red line) captures the relationship between dry core radius and critical supersaturation calculated with the Kappa-Köhler equation (blue line).

S3 Activation emulators

In this study we use the K15 model [1] to estimate the number of formed ice particles N_{ice} in the jet phase of the contrail for different ambient conditions and aircraft exhaust parameters. The amount of activated ice particles is used as input to the Contrail Cirrus Prediction model (CoCiP) [15] which then simulates the evolution of the contrail/contrail cirrus and calculates its energy forcing (EF) if the contrail is persistent. In order to reduce the running time for CoCiP we decided not to run the K15 model during the running of cocip but rather to make an emulator, or activation function, for ice particles based on K15 to use in CoCiP. We generated data from K15 of the fractions of different particle types in the plume forming ice particles for a range of relevant settings to which we fitted functions.

The particles available for contrail formation for hydrogen combustion are limited to ambient aerosols that get entrained into the expanding plume and to emitted lubrication oil particles. For ambient aerosols we chose to generate activation rates for lognormal particle size distributions with mean and standard deviation $\mu_a = 15$ nm, $\sigma_a = 2.2$ and a hygroscopicity set to $\kappa_a = 0.5$. As outlined in the main text the particle size distribution and hygroscopicity of lubrication oil are highly uncertain. Because of the large variations and uncertainties we included a range of values for the mean and standard deviation of the particle size distribution $\mu_o = 525$ nm and $\sigma_o = e^{0.25}$ to $e^1 \approx 1.28$-2.72 in our emulator of lubrication oil activation. The hygroscopicity we kept at the value $\kappa_o = 6 \times 10^{-4}$ regarding this as an upper limit in line with [6] and the mass droplet emission index $\text{EI}_o = 2$ mg (kg fuel)$^{-1}$ when finding the functional form of the emulator. We generated data over a large span of ambient conditions $T_a = 180$-250 K, $p_a = 100$-600 hPa, rh $= 0.1$-1 to be sure to capture all relevant ambient conditions for contrail formation.

The activation of a species of particles l is according to K15 Eq. (40)

$$\begin{aligned}\phi_l &\approx \frac{1}{1+(r_{act,l}/\mu_{r_l})^{\zeta_l}} \\ \zeta_l &= \frac{4}{\sqrt{2\pi}\ln\sigma_l}.\end{aligned} \tag{S5}$$

These expressions are derived in Appendix A in [1]. If there are more particle species than one the activation radius and slope parameter ζ are given by number weighted averages

$$\begin{aligned}\zeta &= \sum_l \phi_l n_{wl}\zeta_l / \sum_l \phi_l n_{wl} \\ r_{act} &= \sum_l \phi_l n_{wl} r_{act,l} / \sum_l \phi_l n_{wl}.\end{aligned} \tag{S6}$$

The expression for the total water droplet number concentration for lubrication oil and ambient aerosols is given by

$$n_w = \phi_o n_{wo} + \phi_a n_{wa}. \tag{S7}$$

n_{wa} is the number concentration of ambient aerosols in the plume which is given by what we call the entrainment factor and the number concentration of ambient aerosols $n_{wa} = E_a n_a$. The ice particle number we get from K15 at the time of quenching of the supersaturation forcing as outlined in the main text and well explained in [1]. We make emulators of ϕ from Eq. (S5) for both lubrication oil and ambient aerosols and in addition the entrainment factor for aerosols at the time of quenching when both are included in the model.

S3.1 Lubrication oil activation emulator

The activation function for lubrication oil A_o is a function of particle size distribution (μ_o, σ_o), ambient temperature T_a, ambient pressure p_a, relative humidity rh, and the critical temperature for fulfilling SAC for contrail formation T_{crit}. The critical temperature in turn is a a function of the ambient pressure. The functional form was found manually by visual inspection and appreciation of known trends, for example for oil particle mean $\mu_o = 5$ nm the activation decreases due to the Kelvin effect. Once a functional form capturing the main features was found parameters were fitted using least squares fit. The emulator for lubrication oil is given below

$$\begin{aligned}&A_o(\mu_o, \sigma_o, T_a, rh, p_a, T_c(p_a)) = \\ &1 - \frac{a}{b(\sigma_o)c(Ta, T_c)} \times \left(1 - \frac{d}{1+e^{-2f(\mu_o,\sigma_o,rh,p_a)g(T_a,rh,T_c)}}\right) \\ &- h(\mu_o, \sigma_o, p_a) - i(\mu_o, \sigma_o, p_a)\end{aligned} \tag{S8}$$

$$
\begin{aligned}
&b(\sigma_o) = 1 + e^{-2b_1(\ln(\sigma_o)-b_2)} \\
&c(T_a, T_c(p_a)) = 1 + e^{-2c_1(T_a - T_c(p_a))} \\
&f(\mu_o, \sigma_o, rh, p_a) = \frac{f_1\mu_o^2(1 - f_2 rh^4)}{(1 + f_3(\sigma_o, p_a))} \\
&f_3(\sigma_o, p_a) = \frac{p_a - 1}{1 + e^{-2f_{31}(\ln(\sigma_o)-f_{32})}} \\
&g(T_a, rh, T_c(p_a)) = T_a - T_c(p_a) + g_1 + g_2 rh^5 \\
&h(\mu_o, \sigma_o, p_a) = h_1(\mu_o)h_2(\sigma_o)h_3(p_a) \\
&h_1(\mu_o) = 1 - \frac{1}{1 + e^{-2h_{11}(\mu_o - h_{12})}} \\
&h_2(\sigma_o) = \frac{1}{1 + e^{-2h_{21}(\ln(\sigma_o)-h_{22})}} \\
&h_3(p_a) = \frac{1}{1 + e^{-2h_{31}(p_a - h_{32})}} \\
&i(\mu_o, \sigma_o, p_a) = i_1 i_2(\mu_o) i_3(\sigma_o) i_4(p_a) \\
&i_2(\mu_o) = 1 - \frac{1}{1 + e^{-2i_{21}(\mu_o - i_{22})}} \\
&i_3(\sigma_o) = i_{31} - \frac{1}{1 + e^{-2i_{32}(\ln(\sigma_o)-i_{33})}} \\
&i_4(p_a) = \frac{1}{1 + e^{-2i_{41}(p_a - i_{42})}}
\end{aligned}
$$

With parameter values

$$
\begin{aligned}
&a = 1.40049540e-01 \\
&b_1 = 7.36579929e+00, b_2 = 6.48662671e-01 \\
&c_1 = 1.51822516e-02, \\
&d = 1.40339479e+00 \\
&f_1 = 1.85507396e-03, f_2 = 3.43463012e-01 \\
&f_{31} = 5.22241740e-01, f_{32} = 6.50965671e-01 \\
&g_1 = -2.29977889e-01, g_2 = 2.06582986e+00 \\
&h_{11} = 1.97979803e-01, h_{12} = 1.00354769e+01 \\
&h_{21} = 4.53390483e+01, h_{22} = 3.70948235e-01 \\
&h_{31} = 8.31021522e-02, h_{32} = 1.32467631e+01 \\
&i_1 = 2.74061220e+01 \\
&i_{21} = 4.40588177e-01, i_{22} = 6.36974326e+00 \\
&i_{31} = 9.56418434e-01, i_{32} = 2.85824957e-01, i_{33} = -4.47149952e+00 \\
&i_{41} = 7.74184182e-01, i_{42} = 1.70779042e+00.
\end{aligned}
\tag{S9}
$$

Even though this is a large and complicated expression it is of course not in complete agreement. Especially activation at low and high air pressures (< 150 hPa and > 350 hPa) for small lubrication oil mean radius are not as accurate as more moderate air pressures or larger mean radius. Contrail formation and persistence however are not as prevalent at these ambient air pressures. Despite the different frequencies of contrail formation at different air pressures we fitted the parameters with equal weight to all air pressures (and relative humidities). This might mean a slightly better fit at these pressures at the expense of a slight reduction in accuracy at moderate air pressures, but also reduces the amount of arbitrary choices in weighting air pressures in the fitting. In Fig. S2 and S3 examples of our lubrication oil activation emulator and results from K15 are shown for all mean radius and standard deviations at $rh = 70\%$ and $p_a = 250$ hPa and the entire span of pressures and relative humidities for $\mu_o = 5$ nm and $\sigma_o = e^{0.25}$ respectively.

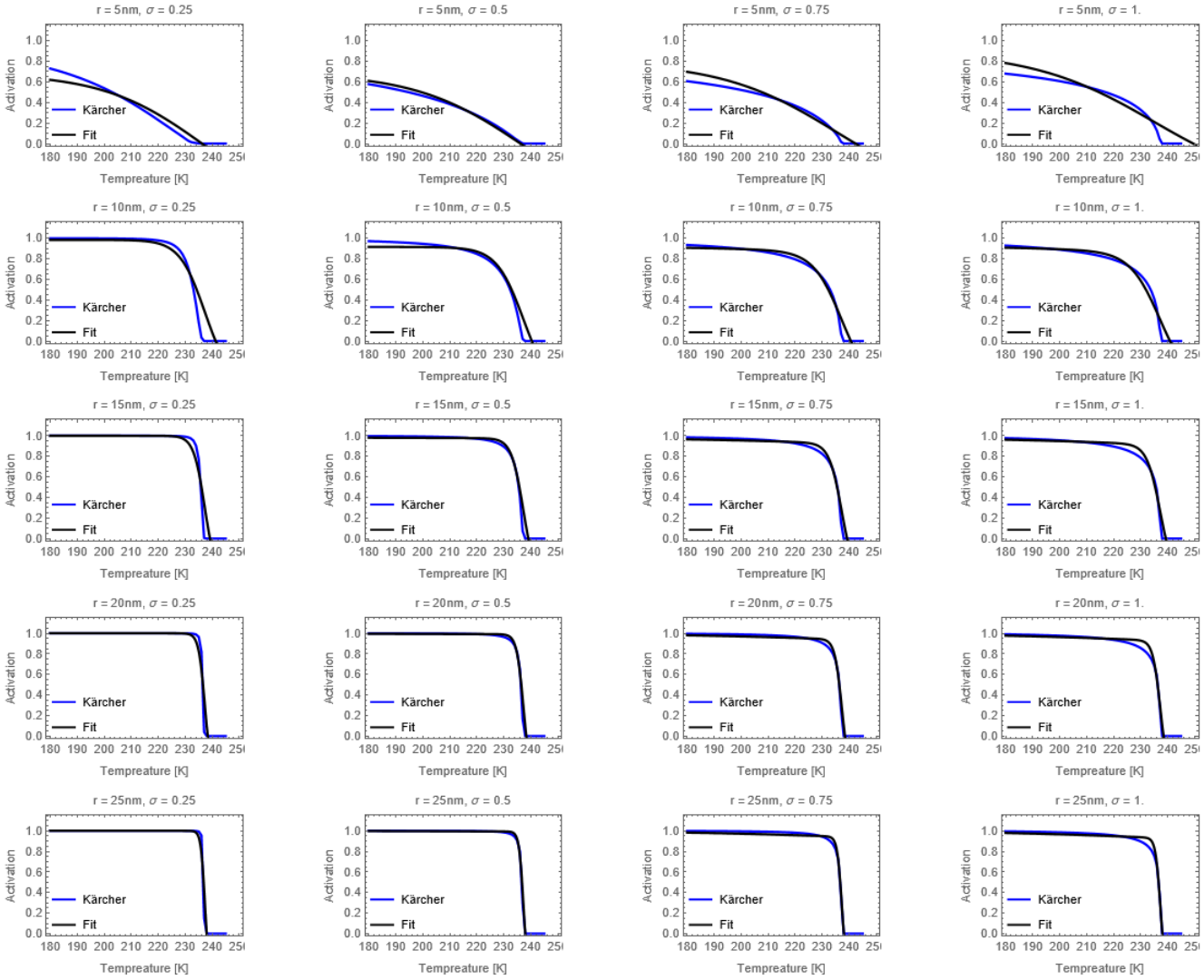

The figure shows examples of how the activation emulator emulates the output from the K15 model for lubrication oil particles over a range of different mean radius and standard deviations at $rh = 70\%$ and $p_a = 250$ hPa.

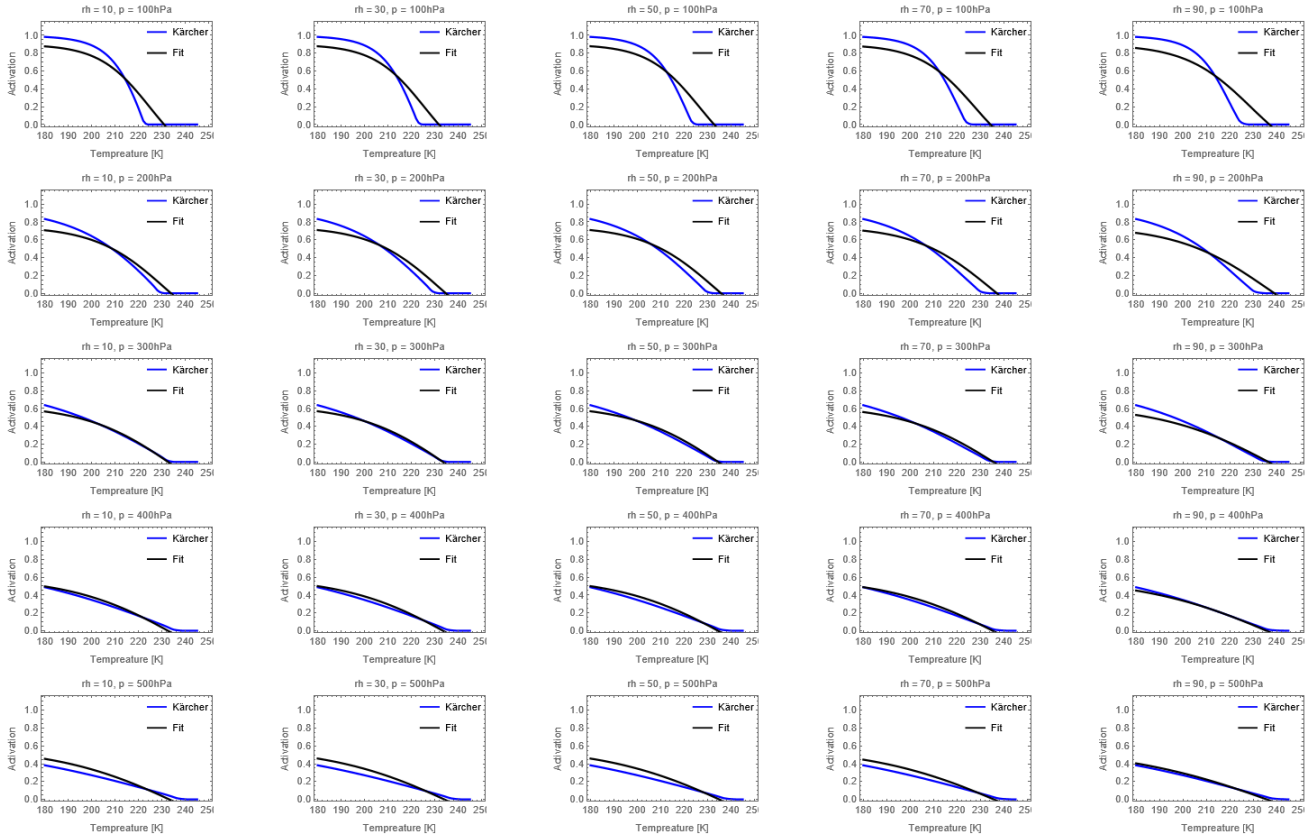

The figure shows examples of how the activation emulator emulates the output from the K15 model for lubrication oil particles for different relatives humidities and pressures for $\mu_o = 5$ nm and $\sigma = e^{0.25}$.

The activation obtained for lubrication oil from K15 depends on the choice of κ_o and EI_o. We chose not to include these variables in our emulator, to not increase the functional complexity further, but the functional form was flexible enough to capture the cases of our sensitivity analysis $\kappa_o = 0.1$ and $\mathrm{EI}_o = 20$ mg (kg fuel)$^{-1}$ with different sets of fitted parameters obtained by a least squares approach. The reason for this is that both the cases of the sensitivity analysis lead to higher activation of the lubrication oil, which are easier patterns to emulate. Below are the parameter settings for the two sensitivity analysis cases $\kappa_o = 0.1$:

$$
\begin{aligned}
&a = 1.83272884e-01 \\
&b_1 = 4.30205937e+00, b_2 = 7.13619714e-01 \\
&c_1 = 3.92789497e-02, \\
&d = 1.52163826e+00 \\
&f_1 = 6.30052888e-03, f_2 = 5.88546882e-01 \\
&f_{31} = 3.78696793e-03, f_{32} = 9.52499644e+01 \\
&g_1 = -2.77310088e-01, g_2 = 7.80894644e-01 \\
&h_{11} = 2.03884382e-01, h_{12} = 2.44892848e+00 \\
&h_{21} = 3.25891968e+00, h_{22} = 4.26092728e-01 \\
&h_{31} = 4.59877098e-01, h_{32} = 2.03479646e+00 \\
&i_1 = 5.57658123e-01 \\
&i_{21} = 4.40588177e-01, i_{22} = 4.88921609e+00 \\
&i_{31} = 6.35705412e-01, i_{32} = 4.55142297e+00, i_{33} = 6.52112505e-01 \\
&i_{41} = 6.75310255e-01, i_{42} = 3.26501727e+00.
\end{aligned}
\tag{S10}
$$

$\mathrm{EI}_o = 20$ mg (kg fuel)$^{-1}$:

$$
\begin{aligned}
&a = 1.13191354e-01 \\
&b_1 = 9.27653785e+00, b_2 = 6.23384277e-01 \\
&c_1 = 6.56666768e-03, \\
&d = 1.32921536e+00 \\
&f_1 = 1.30309620e-03, f_2 = 2.70677254e-01 \\
&f_{31} = 2.27966755e-01, f_{32} = 2.91199176e-01 \\
&g_1 = -6.01952951e-01, g_2 = 2.75490167e+00 \\
&h_{11} = 2.34647173e-01, h_{12} = 1.32130555e+01 \\
&h_{21} = 4.92386286e+01, h_{22} = 3.70439130e-01 \\
&h_{31} = 8.88817482e-02, h_{32} = 1.42979324e+01 \\
&i_1 = 2.02849846e+01 \\
&i_{21} = 3.72701126e-01, i_{22} = 7.16631689e+00 \\
&i_{31} = 9.51619794e-01, i_{32} = 2.83584916e-01, i_{33} = -4.18661787e+00 \\
&i_{41} = 8.69030178e-01, i_{42} = 1.05224846e+00.
\end{aligned}
\tag{S11}
$$

S3.2 Ambient aerosol activation emulator

The emulator for ϕ for ambient aerosols at quench is a function of ambient temperature T_a, pressure p_a, relative humidity rh, and the critical temperature for fulfilling SAC for contrail formation T_{crit} and given by

$$
\phi_{em,a}(T_a, rh, T_c(p_a)) = j_1 \left(1 - \frac{1}{1 + e^{-2(j_2 - rh)(T_a - T_c(p_a))}}\right), \tag{S12}
$$

with parameter values $j_1 = 0.98621099$, $j_2 = 1.27258155$. Included in our activation emulator we have the fraction of ambient aerosols entrained into the plume. In K15 the entrainment is calculated according to their Eq. (37)

$$
\begin{aligned}
E_a &= \frac{T_a}{T}(1 - D) \\
D &= \frac{T - T_a}{T_0 - T_a},
\end{aligned}
\tag{S13}
$$

Where T_0 is the temperature at exhaust. Since the temperature of the plume at quench is unknown we make a fit to the entrainment E_a obtained from the K15 model at quench. Our fit is given by

$$
E_a(\mu_o, T_a, p_a) = k_1(T_a - k_2)^4 - k_3(p_a/10000) + k_4(\mu_o \times 10^9 - k_5) + k_6 \tag{S14}
$$

with parameter values $k_1 = 1.61453153e-10$, $k_2 = 5.76886132e-01$, $k_3 = 3.41028865e-02$, $k_4 = 1.30248424e-03$, $k_5 = 9.72503036e+00$ and $k_6 = 5.19101870e-01$. Here we actually have a slight dependence of the lubrication oil mean radius. Our activation emulator for ambient aerosols is then given by

$$
A_a = E_a \phi_{em,a} \tag{S15}
$$

and shown for all mean radius and standard deviations of lubrication oil at $rh = 70\%$ and $p_a = 250$ hPa in figure S4.

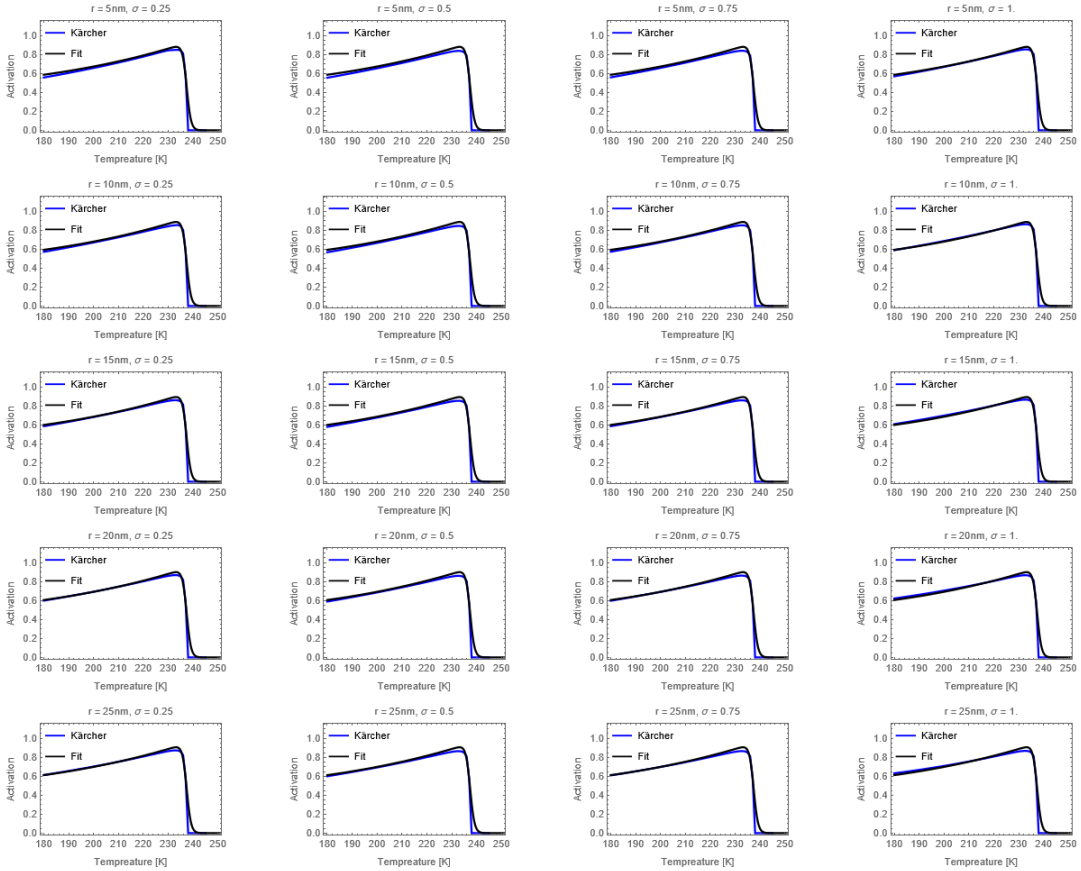

The figure shows examples of how the activation emulator emulates the output from the K15 model for ambient aerosols for different assumptions on lubrication oil particles covering a range of different mean radius and standard deviations at $rh = 70\%$ and $p_a = 250$ hPa

S4 Implementation in CoCiP

To approximate the amount of formed ice particles from soot particles in the original version of CoCiP an unpublished activation function based on raw data from [16] is used

$$A_s(T_a, T_{crit}) = \max(-0.661e^{(T_a - T_c(p_a))} + 1.0, 0). \tag{S16}$$

From the activated soot number emission index, $n_{\text{act,s}} = A_s EI_{\text{n,s}}$ (kg fuel)$^{-1}$, CoCiP calculates the number of activated soot per meter flight according to $N_s = n_{\text{act,s}} \times ff/v_{\text{tas}}$ with the fuel flow ff and true airspeed v_{tas} of the aircraft. This same procedure is used for lubrication oil since we can calculate a lubrication oil number emission index from the mass emission index and Eq. (S2) where a lognormal distribution is assumed [1].

From our emulators based on the K15 model, we get the activation of both lubrication oil and entrained ambient aerosols. For lubrication oil we thus get activated oil per meter flight according to

$$N_o = EI_{n,o} \times A_o \times ff/v_{\text{tas}}. \tag{S17}$$

To get the amount of ice particles formed from ambient aerosols per meter flight in the wake vortex phase we use the expression

$$N_a = E_a \times A_a \times n_a \times n_{\text{engine}} \times A_{\text{plume}}, \tag{S18}$$

where A_{plume} is the cross sectional area of the plume and n_{engine} is the number of engines. For the area of the plume at quench we use a fitted function $A_{\text{plume}}(T_a) = 2 \times 10^{-6}(T_a - 180)^4 + 5$ which is fitted to the area at time of quench from the K15 model. The sum of N_o and N_a give the number of ice particles formed in the jet phase. CoCiPs internal calculation of ice particle loss in the downwash f_{surv} is then used.

S5 Random dates used in sensitivity analysis

Table S3: Twenty randomly selected dates from the year 2019 used in sensitivity analysis simulations.

Month	Days
January	23
February	-
March	22
April	16
May	11
June	3, 13, 26
July	21
August	10, 18, 29
September	9, 19, 27
October	5, 15
November	1
December	18, 20, 25

S6 Comparison of soot activation between Kärcher model and CoCiP

A consistent approach to obtain ice particle numbers for soot when running CoCiP for jet fuel would be to use the K15 model also in this case. We chose instead to use CoCiPs own activation function for soot because of the close similarity in activation (from soot to ice) between the two approaches and simplicity in implementation. CoCiP activates soot particles to ice particles according to Eq. (S16). Activation of soot particles from the K15 model can be seen in Fig. (S5) and CoCiP activation from Eq. (S16) in Fig. (S6) for ambient relative humidities in the span 20-90%, ambient pressures in the span 100-500 hPa and varying ambient temperatures.

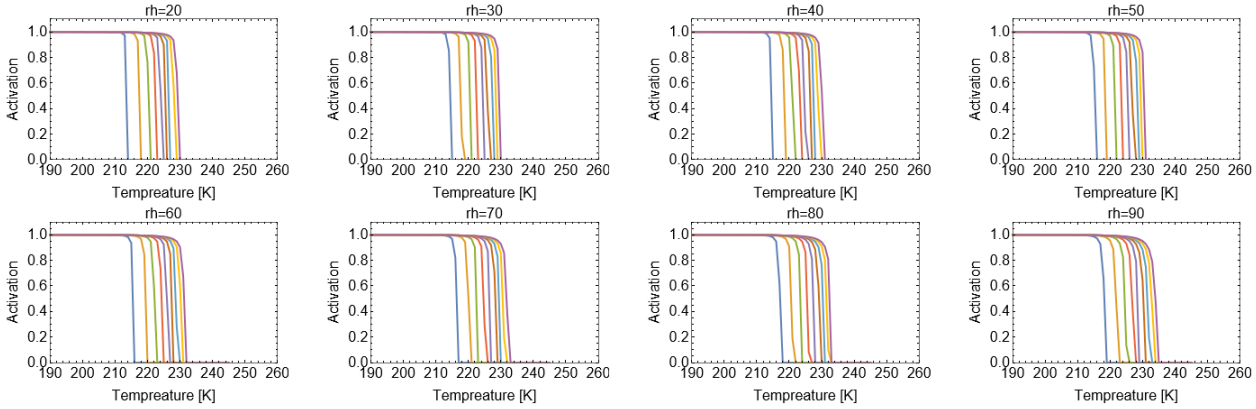

Activation of soot from the K15 model. The different plots show activation of soot for different relative humidities. The different curves in the plot represents different ambient pressures, the blue curve representing the lowest pressure 100 hPa followed by successively higher pressures up to 500 hPa.

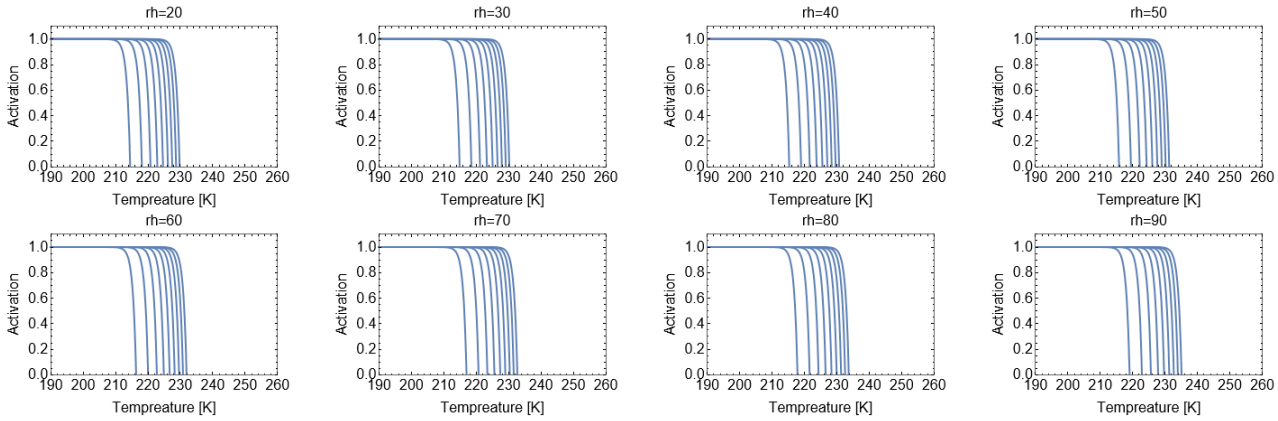

Activation of soot in CoCiP. The different plots show activation of soot for different relative humidities. The different curves in the plot represents different ambient pressures.

References

1. Kärcher, B., Burkhardt, U., Bier, A., Bock, L. & Ford, I. The microphysical pathway to contrail formation. *Journal of Geophysical Research: Atmospheres* **120,** 7893–7927. ISSN: 2169-897X (2015).
2. Patrao, A. C., Jonsson, I., Xisto, C., Lundbladh, A. & Grönstedt, T. Compact heat exchangers for hydrogen-fueled aero engine intercooling and recuperation. *Applied Thermal Engineering* **243,** 122538. ISSN: 1359-4311 (2024).
3. Bier, A. *et al.* Contrail formation on ambient aerosol particles for aircraft with hydrogen combustion: a box model trajectory study. *Atmospheric Chemistry and Physics* **24,** 2319–2344. ISSN: 1680-7316 (2024).
4. Yu, F., Karcher, B. & Anderson, B. E. Revisiting contrail ice formation: Impact of primary soot particle sizes and contribution of volatile particles. *Environmental Science Technology.* ISSN: 0013-936X (2024).
5. Petters, M. & Kreidenweis, S. A single parameter representation of hygroscopic growth and cloud condensation nucleus activity. *Atmospheric Chemistry and Physics* **7,** 1961–1971. ISSN: 1680-7324 (2007).
6. Lambe, A. *et al.* Laboratory studies of the chemical composition and cloud condensation nuclei (CCN) activity of secondary organic aerosol (SOA) and oxidized primary organic aerosol (OPOA). *Atmospheric Chemistry and Physics* **11,** 8913–8928. ISSN: 1680-7324 (2011).
7. Yu, Z. *et al.* Characterization of lubrication oil emissions from aircraft engines. *Environmental science technology* **44,** 9530–9534. ISSN: 0013-936X (2010).
8. Ponsonby, J., King, L., Murray, B. J. & Stettler, M. E. Jet aircraft lubrication oil droplets as contrail ice-forming particles. *Atmospheric Chemistry and Physics* **24,** 2045–2058. ISSN: 1680-7316 (2024).
9. Lewellen, D. C. A large-eddy simulation study of contrail ice number formation. *Journal of the Atmospheric Sciences* **77,** 2585–2604. ISSN: 0022-4928 (2020).
10. Tollmien, W. Berechnung turbulenter ausbreitungsvorgänge. *ZAMM-Journal of Applied Mathematics and Mechanics/Zeitschrift für Angewandte Mathematik und Mechanik* **6,** 468–478. ISSN: 0044-2267 (1926).
11. Kärcher, B. Aviation-produced aerosols and contrails. *Surveys in geophysics* **20,** 113–167. ISSN: 0169-3298 (1999).
12. Goff, J. A. Saturation pressure of water on the new Kelvin temperature scale. *Transactions of the American society of heating and ventilating engineers,* 347–354 (1957).
13. Heating, A. S. o. & Engineers, V. *Transactions of the American Society of Heating and Ventilating Engineers* (The Society, 1925).
14. Murphy, D. M. & Koop, T. Review of the vapour pressures of ice and supercooled water for atmospheric applications. *Quarterly Journal of the Royal Meteorological Society: A journal of the atmospheric sciences, applied meteorology and physical oceanography* **131,** 1539–1565. ISSN: 0035-9009 (2005).

15. Schumann, U. A contrail cirrus prediction model. *Geoscientific Model Development* **5,** 543–580. ISSN: 1991-9603 (2012).

16. Bräuer, T *et al.* Airborne measurements of contrail ice properties—Dependence on temperature and humidity. *Geophysical Research Letters* **48,** e2020GL092166. ISSN: 0094-8276 (2021).